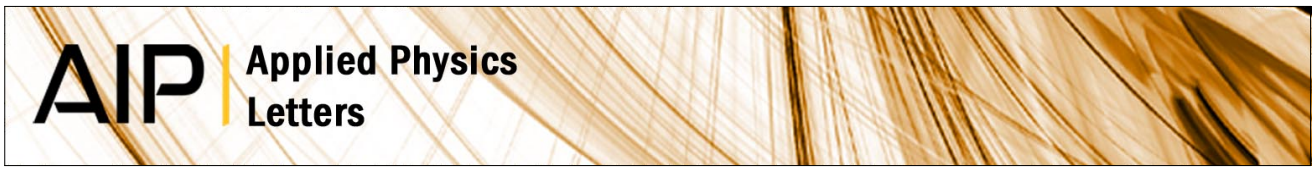

Local atomic and electronic structures and ferroelectric properties of PbZr0.52Ti0.48O3: An x-ray absorption study

S. C. Ray, H. C. Hsueh, C. H. Wu, C. W. Pao, K. Asokan et al.

Citation: Appl. Phys. Lett. **99**, 042909 (2011); doi: 10.1063/1.3607475

View online: http://dx.doi.org/10.1063/1.3607475

View Table of Contents: http://apl.aip.org/resource/1/APPLAB/v99/i4

Published by the American Institute of Physics.

Local atomic and electronic structures and ferroelectric properties of $PbZr_{0.52}Ti_{0.48}O_3$: An x-ray absorption study

S. C. Ray,[1,2,a)] H. C. Hsueh,[1,a)] C. H. Wu,[1] C. W. Pao,[1] K. Asokan,[1,b)] M. T. Liu,[1] H. M. Tsai,[1] C. H. Chuang,[1] W. F. Pong,[1,a)] J. W. Chiou,[3] M.-H. Tsai,[4] J. M. Lee,[5] L. Y. Jang,[6] J. M. Chen,[6] and J. F. Lee[6]

[1]*Department of Physics, Tamkang University, Tamsui 251, Taiwan*
[2]*School of Physics, DST/NRF Centre of Excellence in Strong Materials and Materials Physics Research Institute (MPRI), University of the Witwatersrand, Private Bag 3, WITS 2050 Johannesburg, South Africa*
[3]*Department of Applied Physics, National University of Kaohsiung, Kaohsiung 811, Taiwan*
[4]*Department of Physics, National Sun Yat-Sen University, Kaohsiung 804, Taiwan*
[5]*Department of Electrophysics, National Chiao Tung University, Hsinchu 300, Taiwan*
[6]*National Synchrotron Radiation Research Center, Hsinchu 300, Taiwan*

(Received 28 March 2011; accepted 7 June 2011; published online 29 July 2011; publisher error corrected 3 August 2011)

This work investigates local atomic and electronic structures of $PbZr_{0.52}Ti_{0.48}O_3$ (PZT) thin films with <001>, <101>, and <111> orientations using extended x-ray absorption fine structure (EXAFS) and x-ray absorption near-edge structure (XANES) spectroscopy with $\theta = 0°$ and 70° incident angles. The EXAFS result indicates that the <001>-oriented PZT film has a polarization dominantly along the ***c***-axis, while both <101>- and <111>-oriented PZT films have a dominant in-***ab***-plane polarization. The hysteresis-loop measurements show that the <001>-oriented PZT film has a much larger coercive field than those of other two PZT films, which indicates that the double-well potential along the ***c***-axis is much deeper than that in the ***ab***-plane. © *2011 American Institute of Physics*. [doi:10.1063/1.3607475]

$Pb(Zr_{1-x}Ti_x)O_3$ (PZT) have superior dielectric, piezoelectric, and electromechanical coupling coefficients. The rich structural phase diagram of PZT has attracted much attention because PZT has many potential applications, such as in nonvolatile ferroelectric random access memory.[1] It has a high piezoelectric response in the "morphotropic phase boundary" (MPB) region,[2] in which a transition occurs from the tetragonal to the rhombohedral phase when x is very close to 0.5, and this phase transition depends weakly on the Ti concentration.[3] Yan *et al.*[4] and Utsugi *et al.*[5] prepared tetragonal, monoclinic, and rhombohedral phases of <001>-, <101>-, and <111>-oriented PZT films, respectively, using the $SrRuO_3/SrTiO_3$ (STO) and CaF_2 substrates, respectively, and studied the dependence of their ferroelectric polarizations on the applied electric field. Yan *et al.*[4] observed that the saturation polarization of the <101>-oriented film is the highest, whereas Utsugi *et al.*[5] observed that the saturation polarization of the <001>-oriented film is the highest among the three films considered. García *et al.*[6] observed that the <111>- and <001>-oriented PZT films have the strongest piezo-response along and off the ***c***-axis, respectively. However, these experimental results contradict theoretical calculations of Bellaiche *et al.*,[7] which found that the monoclinic phase, i.e., the phase of the <101>-oriented PZT film has the largest piezoelectric response in PZTs. The extended x-ray absorption fine structure (EXAFS) and x-ray absorption near-edge structure (XANES) experimental techniques are sensitive to the chemical property of the absorbing atom and the bonding with its surrounding ions.[8,9] They are employed here to elucidate the atomic and electronic structures of the PZT films in various orientations and phases as well as their ferroelectric behavior.

Room-temperature EXAFS and XANES measurements at Ti and Zr *K*-edge, Pb L_3-edge, Ti, and Zr $L_{3,2}$-edge were carried out on various beamlines at the National Synchrotron Radiation Research Center, Hsinchu, Taiwan. EXAFS and XANES spectra were measured in the fluorescence mode with two angles of incidence (θ) with respect to the surface normal, which essentially provide measurements in two geometries: (1) $\theta = 0°$ represents normal incidence, where the electric field ***E*** of the linearly polarized photons is parallel to the ***ab***-plane of the film, and (2) $\theta = 70°$ corresponds to grazing incidence, where ***E*** is almost parallel to the ***c***-axis of the film. These geometries will selectively probe in-plane and out-of-plane inter-atomic distances, respectively, in the TiO_6 octahedron. The $PbZr_{0.52}Ti_{0.48}O_3$ (PZT) thin films were prepared by RF magnetron sputtering at room temperature in an argon/oxygen atmosphere and were deposited on LSMO ($La_{0.67}Sr_{0.33}MnO_3$)/STO (<100>), LSMO/Si (<100>), and Pt/Si (<111>) substrates to yield preferentially <001>, <101>, and <111> oriented PZT films as shown by x-ray diffraction (XRD) in Fig. 1(a). According to earlier reports by Yan *et al.*[4] and Utsugi *et al.*,[5] these three PZT films have tetragonal (<001>), monoclinic (<101>), and rhombohedral (<111>) phases, respectively. Fig. 1(b) plots dependence of polarization on the electrical field, i.e., the *P-E* hysteresis loop. Note that the *P-E* hysteresis loop depends on the thermal stress-state and crystallographic characteristics of the PZT thin film so that it varies for the PZT film deposited on different substrates (see Supplementary materials in Ref. 10). Details of preparation and characterization of the samples are available elsewhere.[11]

[a)]Authors to whom correspondence should be addressed: Electronic addresses: raysekhar@rediffmail.com, hsueh@gate.sinica.edu.tw, and wfpong@mail.tku.edu.tw.
[b)]Permanent address: Inter-University Accelerator Centre, Aruna Asaf Ali Marg, New Delhi 110067, India.

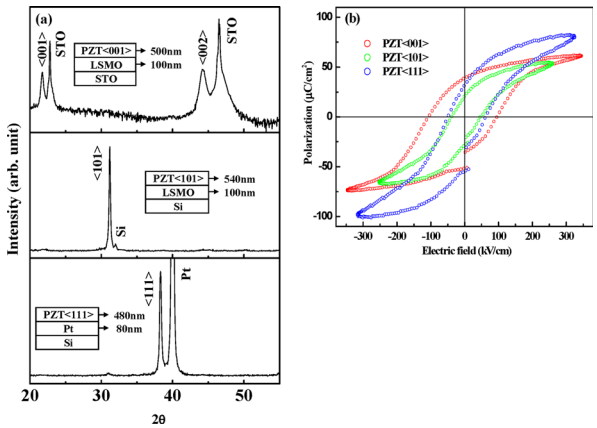

FIG. 1. (Color online) X-ray diffraction pattern of PZT thin films with (a) <001>, <101>, and <111> orientations deposited on LSMO/STO (upper panel), LSMO/Si (middle panel), and Pt/Si (lower panel) substrates, respectively. (b) *P-E* hysteresis loops of PZTs.

Figure 2 presents the Ti *K*-edge XANES spectra of PZTs and reference STO and $PbTiO_3$(PTO). The main absorption edge near 4980 eV in the Ti *K*-edge XANES spectra is due to Ti 1*s* to 4*p* dipole transitions, while the pre-edge structures near 4969-4972 eV were attributed to 1*s* to 3*d* quadrupolar transitions.[3,8,12,13] The pre-edge features are magnified in the lower inset of Fig. 2, which are composed of four features, $\mathbf{P_1}$-$\mathbf{P_4}$, whose intensities vary with the angle of incidence and the phase of PZTs, indicating that the unoccupied density of states (DOSs) of Ti 3*d* are orientation and phase dependent, which are due to that Ti 3*d* orbitals are highly directional. The changes in these XANES spectra are associated with the variation of the local atomic structure of the central Ti atom in the TiO_6 octahedron. Numerous calculations using the modified full multiple scattering method attributed feature $\mathbf{P_1}$ at ~4968 eV to dipole-forbidden but quadruple-allowed $1s \rightarrow 3d\ t^1{}_{2g}e^0{}_g$ transition and attributed features $\mathbf{P_2}$ and $\mathbf{P_3}$ at ~4970.5 and 4973.5 eV to $1s \rightarrow 3d\ t^0{}_{2g}e^1{}_g$ transition.[8] Features $\mathbf{P_2}$ and $\mathbf{P_3}$ at higher energies were also attributed to the *p-d* mixing effect and the transition of the Ti 1*s* electrons to unoccupied 3*d* states of the neighboring transition metal atoms, respectively. The additional feature $\mathbf{P_4}$ observed at an energy higher than that of feature $\mathbf{P_3}$ by ~3eV was argued to occur if there are 4*d* transition metal atoms (such as Zr atoms) inside the octahedrons surrounding the absorbing Ti 3*d* atom.[8] The intensities of these pre-edge features increase with the degree of local structural distortion around the central Ti atom, because the distortion results in 3*d*-4*p* orbital mixing, which enables partial dipole transition to *p-d* hybridized orbitals. Interestingly, features $\mathbf{P_2}$ of <111>- and <101>-oriented PZTs have higher intensities than that of the <001>-oriented PZT. Cao *et al.*[3] observed a similar phenomenon in both <001>- and <111>-oriented PZTs. The variation in the intensity of feature $\mathbf{P_2}$ reflects the fact that the 3*d*-4*p* orbital mixing is strongly affected by ferroelectricity-related *off*-center distortion of the TiO_6 octahedron, which was argued to be a qualitative spectroscopic indication of ferroelectricity in perovskites.[8] Clearly, the intensities of features $\mathbf{P_2}$ of all three <111>- and <101>- and <001>-oriented films for the ***c***-axis ($\theta = 70°$) case exceed those for the ***ab***-plane ($\theta = 0°$) case as shown in the lower inset of Fig. 2, which was argued to suggest that the local atomic structural distortion is larger along the ***c***-axis than in the ***ab***-plane in all three phases of PZTs.[14] In contrast, features $\mathbf{P_3}$ and $\mathbf{P_4}$ exhibit opposite behavior: the intensities of these two features of the <001>-oriented film exceed those of the <111>- and <101>-oriented films. In particular, feature $\mathbf{P_3}$ of the <001>-oriented film becomes wider and merges with feature $\mathbf{P_4}$, which was argued by Vedrinskii *et al.* that the number of Ti 1*s* electron transitions into the unoccupied 3*d* states of neighboring transition metal atoms is higher in the <001>-oriented film than in others.[8] Features $\mathbf{a_1}$ to $\mathbf{c_1}$ attributable to Ti 1*s* electron transitions into the Ti 4*p* unoccupied states of the three PZTs are insensitive to orientation and phase except in intensity. Lee *et al.* observed a similar effect in the $Bi_{4-x}La_xTi_3O_{12}$ film.[15] However, features $\mathbf{a_1}$-$\mathbf{c_1}$ of the <001>-oriented PZT film shift to higher energies by ~1.2 eV relative to those of <101>- and <111>-oriented PZTs. Ravel *et al.* observed similar energy shifts but by a smaller amount in the Ti *K*-edge XANES spectra of PTO and $BaTiO_3$ perovskites and argued that it was due to a smaller charge transfer from Ti to O ions.[9] However, the energy shifts may be also due to the effect of the STO substrate, because they are similar to those of the corresponding features in the Ti *K*-edge XANES spectrum of STO.

The upper insets (a) and (b) in Fig. 2 display the XANES spectra at the Zr *K*-edge and Pb L_3-edge. The general lineshapes of these XANES spectra are almost identical at both the Zr *K*-edge and Pb L_3-edge and are similar to those of reference PTO at the Pb L_3-edge. The distortions of ZrO_6 octahedrons and around Pb sites are difficult to observe in the Zr *K*-edge and Pb L_3-edge XANES spectra[16] due to a large core-hole lifetime broadening in the hard x-ray region. However, the Ti *K*-edge EXFAS spectra (see Supplementary materials and Fig. S1 in Ref. 10) show that the out-of-plane and in-plane Ti-O bond distances differ by ~0.09, 0.10, and 0.19 Å, respectively, for the <001>-, <101>-, and <111>-oriented PZT films. Since the saturation polarization shown in Fig. 1(b) is proportional to the product of the *off*-center displacement of the Ti/Zr ions and the effective charge on the Ti/Zr ion, these Ti-O bond-distance differences suggest that the

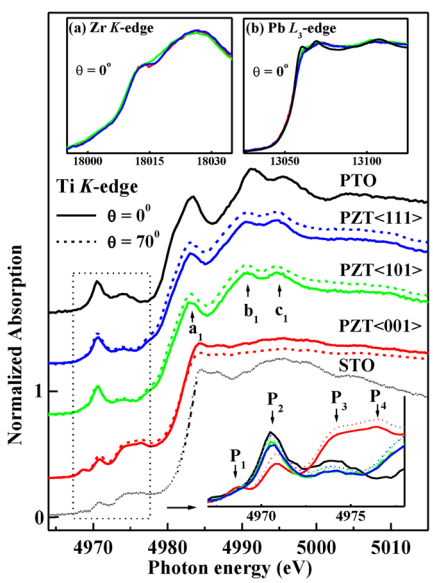

FIG. 2. (Color online) Normalized polarization-dependent Ti *K*-edge XANES spectra of PZTs and reference PTO and STO. Insets (a) and (b) present Zr *K*-edge and Pb L_3-edge XANES spectra, respectively, of all PZTs and PTO obtained at $\theta = 0°$.

<111>-oriented PZT film has the largest saturation polarization, while the saturation polarizations of <001>- and <101>-oriented PZT films are comparable, which indeed agree with the saturation polarizations shown in their respective hysteresis loops [Fig. 1(b)]. The hysteresis loops shown in Fig. 1(b) also reveal that the coercive fields for the <101>- and <111>-oriented PZT films are comparable, while that of the <001>-oriented PZT film is considerably larger, which may be due to differing domain structures in these films.

Figure 3(a) shows Ti $L_{3,2}$-edge XANES spectra of PZTs and reference PTO and STO. The spectra of PZTs include two features denoted as $\mathbf{a_2}$ and $\mathbf{b_2}$ in the L_3-edge and two features denoted as $\mathbf{c_2}$ and $\mathbf{d_2}$ in the L_2-edge. The separation between L_3 and L_2 edges is due to spin-orbit coupling, which splits the Ti $2p$ core state into Ti $2p_{3/2}$ (L_3) and $2p_{1/2}$ (L_2) by about 5.5 eV similar to those of other perovskites.[17] Ti $3d$ band at both L_3- and L_2-edge split into t_{2g} and e_g sub-bands with a ~2.5 eV separation by the crystal field, which depends on the polarization.[18] The main difference between the absorption spectra of PZTs and PTO is that the double structure of PTO (indicated by two solid bars) becomes a single feature $\mathbf{b_2}$ of PZTs. Features $\mathbf{b_2}$ and $\mathbf{d_2}$ associated with the e_g states of the <101>- and <111>-oriented films are shifted to the higher energy side by 0.4 eV from those of the <001>-oriented film. The spectrum of the <001>-oriented film has the highest intensity, while the spectrum of the <111>-oriented film has the smallest intensity. The e_g states are composed of d_{z^2} and $d_{x^2-y^2}$ orbitals, which are directional and point toward ligand anions, so that they depend on the deviation of the Ti octahedral symmetry.[19] The similarity between the e_g states of PZTs and STO indicates that the distortion from the octahedral symmetry in PZTs is reduced, because STO has a high degree of octahedral symmetry. This result suggests that the Ti atom in PZTs has a better octahedral symmetry than that in PTO. Fig. 3(b) presents Zr $L_{3,2}$-edge XANES spectra of PZTs. Because of the dipole-transition selection rule, the Zr $L_{3,2}$-edge absorption features reflect local DOSs with s and d characters. The features denoted as $\mathbf{a_3}$ and $\mathbf{b_3}$ in the L_3-edge and as $\mathbf{c_3}$ and $\mathbf{d_3}$ in the L_2-edge are primarily due to the splitting of the Zr $4d$ orbitals into t_{2g} and e_g orbitals at an octahedral site similar to those of the Ti atom in the TiO_6 octahedron. However, unlike those features at the Ti $L_{3,2}$-edge, the <101>-oriented film yields the highest intensity than those of the <001> and <111>-oriented film, indicating that the <101>-oriented film has maximum unoccupied DOSs. Feature $\mathbf{b_3}$ of the e_g states in the <101>-oriented film also shifts downward in energy by ~0.5 eV as shown in the inset of Fig. 3(b). This result may be related to the different mean size of the ZrO_6 and TiO_6 octahedrons[3] for ZrO_6 octahedrons in PZTs are less distorted. The degree of hybridization and charge transfer between Zr $4d$ and O $2p$ differs from those of Ti $3d$ and O $2p$ in TiO_6 octahedrons.

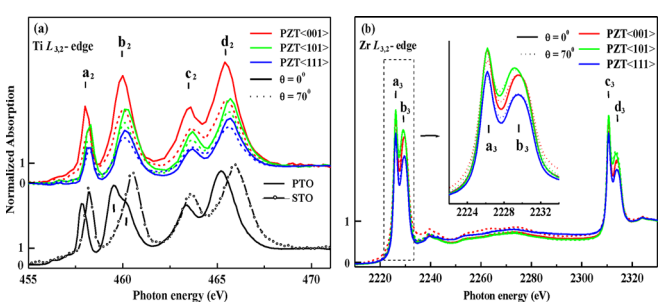

FIG. 3. (Color online) (a) Normalized polarization-dependent Ti $L_{3,2}$-edge XANES spectra of PZTs and reference PTO and STO. (b) Normalized Zr $L_{3,2}$-edge XANES spectra of PZTs. Inset magnifies Zr L_3-edge XANES spectra.

To elucidate the polarization effects of PZT polymorphisms, we have performed Born effective charge calculations of these three PZTs in tetragonal, monoclinic, and rhombohedral phases within the density functional perturbation theory as implemented in ABINIT package.[20] The local density approximation is employed to describe the electronic exchange-correlation interactions and the electronic configurations of Pb ($5d^{10}$, $6s^2$, $6p^2$), Zr ($4d^2$, $5s^2$), Ti ($3d^2$, $4s^2$), and O ($2s^2$, $2p^4$) are treated as valence states to generate pseudopotentials in FHI code.[21] The cutoff energy up to 80 Ha for the plane wave basis set expansion was used. The underlying atomic positions of the optimized lattice constants for three phases ($\boldsymbol{a} = \boldsymbol{b} = 7.64$ a.u. and $\boldsymbol{c} = 15.62$ a.u. for tetragonal phase; $\boldsymbol{a} = 10.79$ a.u., $\boldsymbol{b} = 10.77$ a.u. and $\boldsymbol{c} = 7.82$ a.u. for monoclinic phase; $\boldsymbol{a} = \boldsymbol{b} = \boldsymbol{c} = 15.28$ a.u. for rhombohedral phase) are relaxed under the first-principles calculated atomic forces. The calculated diagonal elements of the Born effective-charge tensors of the representative cations are tabulated and given in the supplementary part (see Table I in Ref. 10) and compared with previous PZO/PTO superlattice calculation.[22] Table I shows that the effective charges of the Ti ion in the tetragonal, monoclinic, and rhombohedral phases, corresponding to <001>-, <101>-, and <111>-oriented PZT films, respectively, are comparable, though they show a trend as monoclinic > tetragonal > rhombohedral. This trend disagrees with that inferred from the *P-E* hysteresis-loop measurements and the Ti *K*-and $L_{3,2}$-edge XANES data, which show a trend of tetragonal > monoclinic ~ rhombohedral. This discrepancy may be due to the use of a defect-free bulk model in the calculation. However, a realistic structural model, which includes the effects of substrate, defects and surface is beyond the capability of the present work.

[1]O. Auciello *et al.*, Phys. Today **51**(1), 22 (1998).
[2]N. Ledermann *et al.*, Sens. Actuators A **105**, 162 (2003).
[3]D. Cao *et al.*, Phys. Rev. B **70**, 224102 (2004).
[4]L. Yan *et al.*, Appl. Phys. Lett. **89**, 262905 (2006).
[5]S. Utsugi *et al.*, Appl. Phys. Lett. **96**, 102905 (2010).
[6]R. E. García *et al.*, J. Appl. Phys. **100**, 064105 (2006).
[7]L. Bellaiche *et al.*, Phys. Rev. Lett. **84**, 5427 (2000).
[8]R. V. Vedrinskii *et al.*, J. Phys.: Condens. Matter **10**, 9561 (1998).
[9]B. Ravel and E. A. Stern, Physica B **208–209**, 316 (1995).
[10]See supplementary material at http://dx.doi.org/10.1063/1.3607475 for the discussion of stress dependence of electrical properties and crystallographic characteristics, Fourier transform of the Ti *K*-edge EXAFS and calculated Born effective charges of the cations in PZT in three different crystal structures.
[11]S. C. Ray *et al.*, Mat. Lett. **60**, 1714 (2006).
[12]N. Jiang *et al.*, Phys. Rev. B **76**, 214117 (2007).
[13]V. R. Mastelaro *et al.*, J. Appl. Phys. **105**, 033508 (2009).
[14]U. Chon *et al.*, Phys. Rev. Lett. **89**, 087601 (2002).
[15]D. W. Lee *et al.*, J. Appl. Phys. **99**, 034101 (2006).
[16]I. Grinberg *et al.*, Nature **419**, 909 (2002).
[17]J. C. Jan *et al.*, Appl. Phys. Lett. **87**, 012103 (2005).
[18]T. Higuchi *et al.*, Jap. J. Appl. Phys. **44**, L1491 (2005).
[19]P. Nachimuthu *et al.*, J. Phys. Chem. B **109**, 1337 (2005).
[20]X. Gonze and C. Lee, Phys. Rev. B **55**, 10355 (1997).
[21]M. Fuchs and M. Scheffler, Computer Phys. Commun. **119**, 67 (1999).
[22]C. Bungaro and K. M. Rabe, Phys. Rev. B **65**, 224106 (2002).